Distribution of Energy Flow by Dielectric Waveguide with Deformed Rhombic Dielectric Structure along a Middle Layer

Ryosuke Ozaki[#1], Tsuneki Yamasaki[#2]

[#] *College of Science and Technology, Nihon University*
1-8-14, Surugadai Kanda Chiyoda-ku, Tokyo, 101-8308, Japan.
[1]ozaki@ele.cst.nihon-u.ac.jp, [2]yamasaki@ele.cst.nihon-u.ac.jp

Abstract—**In this paper, we have analyzed the guiding problem by dielectric waveguide with defects area composed of dielectric circular cylinder array loaded with deformed rhombic dielectric structure in the middle layer, and investigated the influence of the distribution of energy flow for defect area by using the propagation constants of the guided region. Numerical results are given for the complex propagation constants and distribution of enegy flow for case of comparison of both rhombic dielectric structure and deformed rhombic dielectric structures by using the combination of improved Fourier series expansion method and multilayer method. As numerical results, it is shown that we can be obtained the confinement efficiency by rhombic dielectric structure compared with defomed rhombic dielectric structures for TE and TM modes.**

I. INTRODUCTION

Optical wave propagation in the periodic structure such as photonic crystals structure[1],[2] has been both theoretical and practical interest in many areas physics and engineering. In general, photonic crystals such as optical nanostructures with periodically permittivity distribution are known as technology which can be controlled the light in the periodic structure by the interaction of both the wave nature of light and periodicity. They have expected the development in integrated optics and optoelectronics fields. Therefore, in the design of photonic crystals structure, it is very important to investigate the stop band regions or photonic band gaps. As these applications, for example, there are optical devices such as an optical coupler, optical resonator, and optical waveguide filter. However, it is not analyzed the stop band region in Bragg region in detailed, many numerical results are shown only the distribution of electromagnetic fields by utilizing the FDTD method, TD-BPM method, and another numerical techniques[3]-[6].

In recent paper[7]-[9], we have analyzed the guiding problem by dielectric waveguide with defects layer composed of dielectric circular cylinder array loaded with dielectric circular cylinder or rhombic dielectric structure in the middle layer, and investigated the influence of propagation constants near the stop band regions and distribution of energy flow for TE and TM modes. As numerical results, it is denoted that we can be concentrated the energy into the defect area by rhombic dielectric structure or dielectric circular cylinder for TM and TE mode, respectively. We have considered that proposed analytical model would like to apply the devices such as an optical resonator. Therefore, we have investigated the optimum dielectric waveguide with arbitrary inhomogeneous media in the middle layer so that the energy can almost concentrate into the defects area.

In this paper, we have analyzed the guiding problem by dielectric waveguide with defects area composed of dielectric circular cylinder array loaded with deformed rhombic dielectric structure in the middle layer and investigated the influence of the distribution of energy flow for defect area by using the propagation constants of the guided region.

Numerical results are given for the complex propagation constants and the distribution of energy flow for case of comparison of both rhombic dielectric structure and deformed rhombic dielectric structures by using the combination of improved Fourier series expansion method and multilayer method. As numerical results, it is shown that we can be obtained the confinement efficiency by rhombic dielectric structure compared with deformed rhombic dielectric structures for TE and TM modes.

II. METHOD OF ANALYSIS

We consider the dielectric waveguides with deformed rhombic dielectric structure as shown in Fig.1. The structure ($D = Ld$) shown in the figure is periodic with a period p along the z-direction and uniform in the y-direction. The configuration as shown in figure has dielectric circular cylinders with radius a and $d_1/2$ in the x- and z-directions, respectively. The permittivity of regions S_1 and S_3 are defined by dielectric constants ε_0 and that of circular cylinder array in the periodic length is denoted by ε_a , ε_b , and ε_3 . The middle layer region has only deformed rhombic dielectric cylinder with parameters b and c in the x- and z-directions and dielectric constants $\varepsilon_3^{(m)}$. The thickness of each layer is defined by d , and diameter of circular cylinder is defined by d_1 . The permeability is assumed to be μ_0 in all regions. The time dependence $\exp(-i\omega t)$ in the field expresion will be omitted.

In the formulation, TE case is discussed and the TM case only numerical results are presented. The electric fields in the regions $S_1(x \geq 0)$ and $S_3(x \leq -D)$ are expressed as[7]-[9]
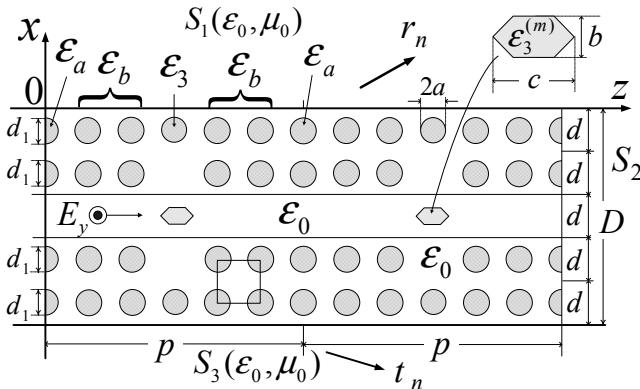
Fig.1. Structure of dielectric waveguide with deformed rhombic dielectric cylinder along a middle layer

$$E_y^{(1)} = e^{i\gamma z} \sum_{n=-N}^{N} r_n \exp\{ik^{(n)}x + i2n\pi z/p\}, \tag{1}$$

$$E_y^{(3)} = e^{i\gamma z} \sum_{n=-N}^{N} t_n \exp\{-ik^{(n)}(x+D) + i2n\pi z/p\}, \tag{2}$$

$$k^{(n)} \triangleq \sqrt{k_0^2 - (\gamma + 2\pi n/p)^2}, \quad k_0 \triangleq \omega\sqrt{\varepsilon_0\mu_0} = 2\pi/\lambda, \tag{3}$$

where $\gamma(\triangleq \beta + i\alpha; \alpha > 0)$ and $k^{(n)}$ are the propgation constans in the z- and x-directions, respectively. k_0 is the wave number, λ is the wavelength in free space. r_n and t_n are unknown coefficients to be determined from boundary conditions. The sign of $k^{(n)}$ are given by the radiation condition in guiding problem. In the region $S_2(-D < x < 0)$, the first layer $(-d < x < 0)$ is divided into M this layers and the permittivity profile in each layer ($d_\Delta \triangleq d/M$) is approximated by step index profile $\varepsilon^{(l)}(z)$. Using the eigenvalue $h_\nu^{(l)}$ and eigenvector $u_{\nu,n}^{(l)}$ found from eigenvalue equation, the electromagnetic fields can be expanded as finite Fourier series[7]-[9].

$$E_y^{(2,l)} = \sum_{\nu=1}^{2N+1} [A_\nu^{(l)} e^{-ih_\nu^{(l)}\{x+(l-1)d_\Delta\}} + B_\nu^{(l)} e^{ih_\nu^{(l)}(x+ld_\Delta)}] f_\nu^{(l)}(z), \tag{4}$$

$$f_\nu^{(l)}(z) \triangleq e^{i\gamma z} \sum_{n=-N}^{N} u_{\nu,n}^{(l)} e^{i2\pi nz/p}, \quad 1 \le l \le M, \tag{5}$$

$$H_x^{(2,l)} \triangleq \frac{-1}{i\omega\mu_0}\frac{\partial E_y^{(2,l)}}{\partial z}, \quad H_z^{(2,l)} \triangleq \frac{1}{i\omega\mu_0}\frac{\partial E_y^{(2,l)}}{\partial x}, \tag{6}$$

where $A_\nu^{(l)}$ and $B_\nu^{(l)}$ are unknown coefficients to be determined from boundary conditions. Using the boundary conditions at $x = -ld_\Delta (l = 1 \sim M-1)$, we can be obtained the matrix relational equation between $\mathbf{A}^{(1)}, \mathbf{B}^{(1)}$ and $\mathbf{A}^{(M)}, \mathbf{B}^{(M)}$ by matrix algebra[7]-[9].

$$\begin{pmatrix} \mathbf{A}^{(1)} \\ \mathbf{B}^{(1)} \end{pmatrix} = \begin{pmatrix} \mathbf{S}_1 & \mathbf{S}_2 \\ \mathbf{S}_3 & \mathbf{S}_4 \end{pmatrix} \begin{pmatrix} \mathbf{A}^{(M)} \\ \mathbf{B}^{(M)} \end{pmatrix}, \tag{7}$$

We apply the matrix relation for another layer by utilizing in Eq.(7) except the permittivity profile, and considered the
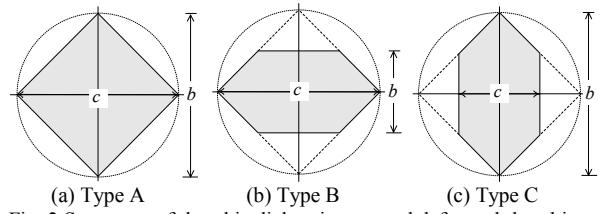

Fig. 2 Structures of rhombic dielectric type and deformed rhombic dielectric types in the middle layer

symmetric structure, we can be obtained the following equations, respectively[7]-[9]:

$$\begin{pmatrix} \mathbf{A}^{(1)} \\ \mathbf{B}^{(1)} \end{pmatrix} = \begin{pmatrix} \mathbf{S}_1^{(U)} & \mathbf{S}_2^{(U)} \\ \mathbf{S}_3^{(U)} & \mathbf{S}_4^{(U)} \end{pmatrix} \begin{pmatrix} \mathbf{A}^{(3M)} \\ \mathbf{B}^{(3M)} \end{pmatrix}, \tag{8}$$

$$\begin{pmatrix} \mathbf{A}^{(5M)} \\ \mathbf{B}^{(5M)} \end{pmatrix} = \begin{pmatrix} \mathbf{S}_1^{(L)} & \mathbf{S}_2^{(L)} \\ \mathbf{S}_3^{(L)} & \mathbf{S}_4^{(L)} \end{pmatrix} \begin{pmatrix} \mathbf{A}^{(3M)} \\ \mathbf{B}^{(3M)} \end{pmatrix}. \tag{9}$$

Rearranging the unknown coefficients in regard to $\mathbf{A}^{(3M)}$ in the middle layer, substituting Eqs.(8) and (9) into the boundary conditions at $x = 0$ and $x = -D$, we can be obtained the following equation[7]-[9]:

$$\mathbf{W} \cdot \mathbf{A}^{(3M)} = \mathbf{0}. \tag{10}$$

For a nontrivial solution to exist in Eq.(10), we have the following characteristics equation[7]-[9]:

$$\det(\mathbf{W}) = 0. \tag{11}$$

The propagation constants γ can be evaluated by utilizing the Muller's method to compute in Eq.(11). To analyze the distribution of energy flow by using the propagation constants of the guided area found from in Eq.(11), the Poynting vector is defined by following equation[7]-[9]:

$$\mathbf{S} \triangleq \mathbf{a}_x S_x + \mathbf{a}_z S_z, \tag{12}$$

where $\mathbf{a}_x$ and $\mathbf{a}_z$ are the unit vector in the x and z-directions, respectively. In the electromagnetic fields of the middle layer, by setting with $A_{\nu=1}^{(l=l_m)} = 1$ at the center layer ($l_m \triangleq (M+1)/2$) of the middle layer, the unknown coefficients are given by the ration of $A_{\nu\neq1}^{(l)}/A_{\nu=1}^{(l)}$ from Eq.(10). Then, unknown coefficients $A_{\nu\neq1}^{(l=l_m)}, B_{\nu\neq1}^{(l=l_m)}$ for the electromagnetic fields can be evaluated by solving the simultaneous equation at $l = l_m$. In the case of another layer for the middle layer, it can be obtained by using the boundary conditions. To analyze the distribution of energy flow, the magnetic fields are given by Eq.(6). Where, the components of Poynting vector are given by following equations:[7]-[9]

$$S_x^{(TE)} \triangleq \text{Re}\left[E_y^{(2,l)} \times \{H_z^{(2,l)}\}^*\right]/2, \tag{13}$$

$$S_z^{(TE)} \triangleq \text{Re}\left[E_y^{(2,l)} \times \{H_x^{(2,l)}\}^*\right]/2. \tag{14}$$

The distribution of energy flow in the numerical results are evaluated by the following equation[7]-[9].

$$P^{(TE)} \triangleq \sqrt{\{S_x^{(TE)}\}^2 + \{S_z^{(TE)}\}^2}. \tag{15}$$

where the superscripts (TE) mean the TE mode case.
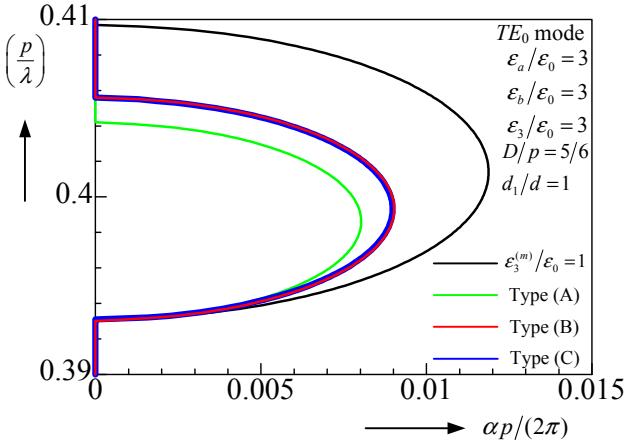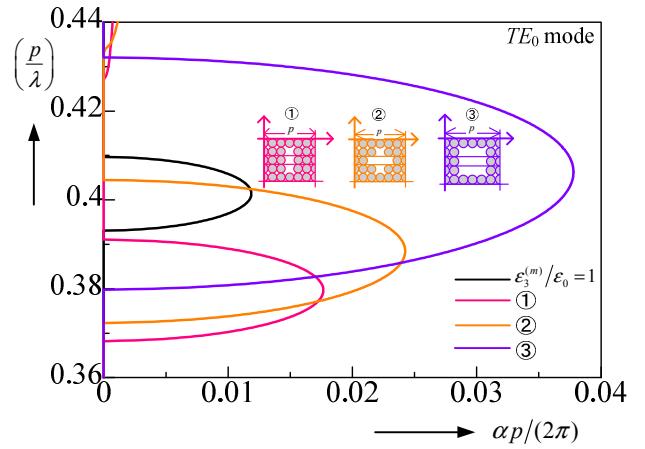
(a) comparison of types A, B, and C   (b) comparison of model ①, ②, and ③

Fig.3. Normalized attenuation constants vs. normalized frequency for TE mode

(a) Type A   (b) Type B   (c) Type C
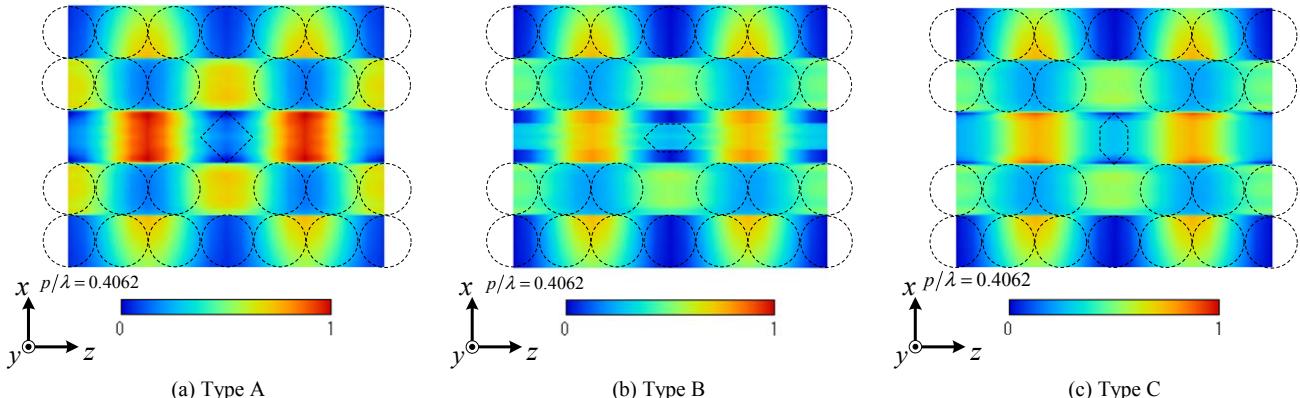
Fig. 4. Distribution of energy flow $P^{(TE)}$

III. NUMERICAL RESULTS

We consider the lowest guided TE_0 and TM_0 modes ($0 < p/\lambda < 0.5$), and the structure based on the circular cylinders as rhombic dielectric structure types in the middle layer as shown in Fig.2. The structure of deformed rhombic dielectric has parameters $c/p = 1/6$, $b/d = 0.5$ for type B and $c/p = 1/12$, $b/d = 1.0$ for type C. The values of parameter chosen are $\varepsilon_a/\varepsilon_0 = 3$, $\varepsilon_b/\varepsilon_0 = 3$, $\varepsilon_3/\varepsilon_0 = 3$, $d_1/d = 1$, $D/p = 5/6$. The numerical computation in this paper is performed using the truncation number $N = 10$ or $N = 9$ for TE and TM modes and $M = 41$ which make the relative error to the extrapolated true values less than about 1%.

Figure 3(a) shows the normalized attenuation constants ($\alpha p/(2\pi)$) versus normalized frequency (p/λ) for various types in the middle layer as condition of $\varepsilon_3^{(m)}/\varepsilon_0 = 3$ for TE_0 mode. Figure 3(b) show the $\alpha p/(2\pi)$ versus p/λ for various resonator structures ①, ②, and ③ as shown in this figure except the black solid line of $\varepsilon_3^{(m)}/\varepsilon_0 = 1$. The black solid line of $\varepsilon_3^{(m)}/\varepsilon_0 = 1$ is the result as case of air region in the middle

layer for both figures 3(a) and 3(b). From these figure 3(a) and 3(b), we can see the following features:

(1) The stop band region of type A is shifted the lower normalized frequency than that of types B and C. Because of equivalent permittivity is increased.

(2) As the equivalent dielectric constant of types B and C is same, the property of type B is almost equal to that of type C.

(3) The stop band region of the structure ③ is covered that of other types A, B, and C.

Using propagation constants of the guided area, figures 4(a), 4(b), and 4(c) show the distribution of energy flow for types A, B, and C in the middle layer as condition of same excited normalized frequency $p/\lambda = 0.4062$. From these figures, we can see the following features:

(1) A tendency of distribution for type B is similar to that of type C. As a reason of this resutls, we have a think that because of using the same propagation constant for both type B and type C.

(2) The energy of defect area can be concentrated than that of types B and C.

Similaly, figures 5(a) and 5(b) show the $\alpha p/(2\pi)$ versus p/λ for various types in the middle layer as condition of $\varepsilon_3^{(m)}/\varepsilon_0 = 3$ and for various resonator structures ①, ②, and
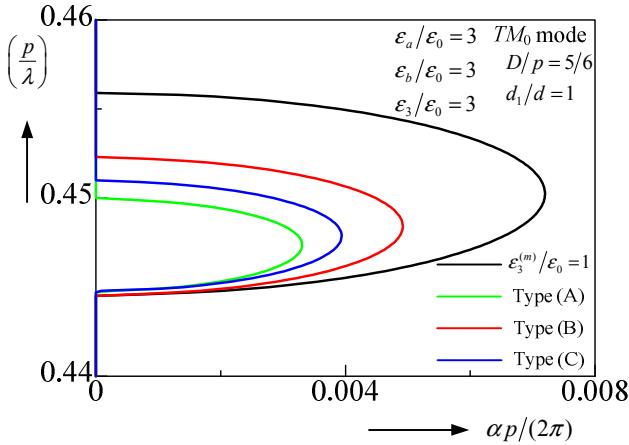
(a) comparison of types A, B, and C
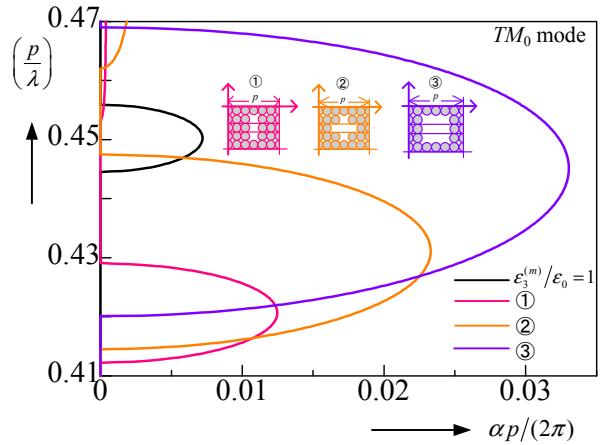
(b) comparison of model ①, ②, and ③

Fig. 5. Normalized attenuation constants vs. normalized frequency for TM mode

(a) Type A

(b) Type B

(c) Type C
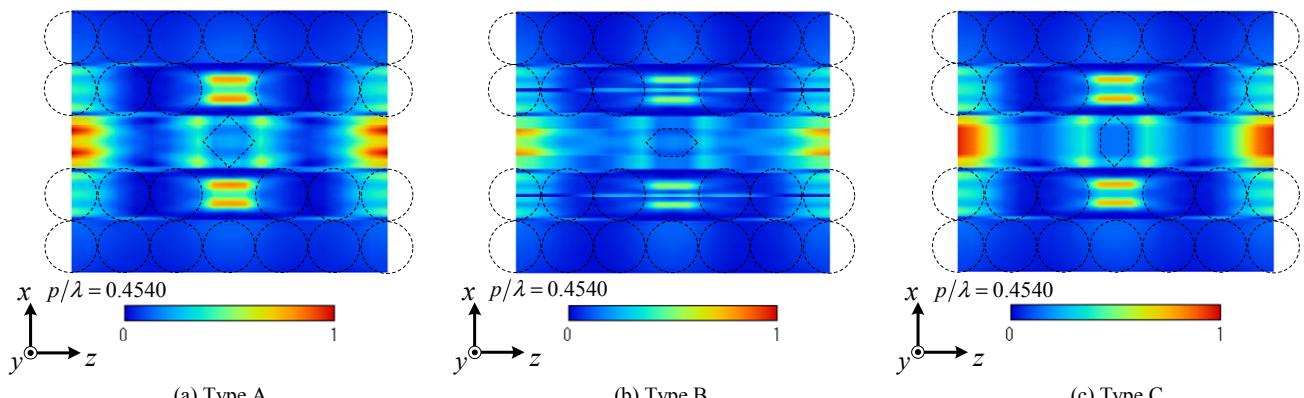
Fig. 6. Distribution of energy flow $P^{(TM)}$

③ for TM mode, respectively. From these figures 5, although a tendency of property becomes the same as the case of TE mode, we can see that the property of types B and C is different because of the influence of polarization.

Figures 6(a), 6(b), and 6(c) show the distribution of energy flow for types A, B, and C in the middle layer for $\varepsilon_3^{(m)}/\varepsilon_0 = 3$ as condition of same excited normalized frequency $p/\lambda = 0.4540$ using the propagation constants of the guided area. From these figures, we can see the following features:

(1) By the comparison of type B and type C, it can be obtained the energy can be concentrated in the defect area.

(2) By the comparison of type A and C, the energy in the defect area for type A can be concentrated than case of type C.

IV. CONCLUSION

In this paper, we have analyzed the guiding problem for dielectric waveguide with defects area composed of dielectric circular cylinder array loaded with deformed rhombic dielectric structure along a middle layer by using the combination of improved Fourier series expansion method and multilayer method, and investigated the distribution of energy flow for defects area by utilizing the propagation constants of the guided regions for both TE_0 and TM_0 mode.

REFERENCES

[1] J. D. Joannopoulos, S. G. Johnson, J. N. Winn, and R. D. Meade, *Photonic Crystals: Molding the Flow of Light*, 2nd ed., Princeton University Press, Princeton and oxford, 2008.
[2] K. Sakoda, *Optical Properties of Photonic Crystals,* 2nd ed., Springer-Verlag, 2005.
[3] K. Yasumoto, Ed., *Electromagnetic Theory and Applications for Photonic Crystals*, CRC Press, 2005.
[4] Y. Naka and H. Ikuno, "Two-dimensional photonic crystal L-shaped bent waveguide and its application to wavelength multi/demultiplexer," *Truk. J. Elec. Engin.,* vol. 10, no. 2, pp.245–256, 2002.
[5] M. Koshiba, Y. Tsuji, and M. Hikari, "Time-domain beam propagation method and its allication to photonic crystal circuits," *J. Light. Tech.*, vol. 18, no. 1, pp.102–110, Jan. 2000.
[6] A. Adibi, Y. Xu, R. K. Lee, A. Yariv, and A. Scherer, "Properties of the slab modes in photonic crystal optical waveguides," *J. Light. Tech.*, vol. 18, no.11, pp. 1554–1564, Nov. 2000.
[7] R. Ozaki and T. Yamasaki, "Propagation characteristics of dielectric waveguides with arbitrary inhomogeneous media along the middle layer," *IEICE Trans. Electron.*, vol. E95-C, no.1, pp. 53–62, Jan. 2012.
[8] R. Ozaki and T. Yamasaki, "Distribution of energy flow by dielectric waveguide with rhombic dielectric structure along a middle layer," *IEICE Electron. Exp.*, vol. 9, no. 7, pp. 698–705, April, 2012.
[9] R. Ozaki and T. Yamasaki, "Distribution of energy flow by dielectric waveguide with rhombic dielectric structure along a middle layer – Case of Compared with deformed rhombic dielectric structure – ," *IEICE Trans. Electron.*, vol. E96-C, no.1, Jan. 2013.(to be published)